Vacuum xxx (2016) 1–6

Contents lists available at ScienceDirect

Vacuum

journal homepage: www.elsevier.com/locate/vacuum

Influence of Cr_2O_3 thickness on the magnetic properties of NiFe/Cr_2O_3 bilayers deposited on $SiTrO_3$ single-crystalline substrate

Yu-Chi Chang [a], Xu Li [b], Ryan D. Desautels [c], Ko-Wei Lin [a, *], Johan van Lierop [c, **], Antonio Ruotolo [d], Philip W.T. Pong [b, ***]

[a] Department of Materials Science and Engineering, National Chung Hsing University, Taichung 402, Taiwan
[b] Department of Electrical and Electronic Engineering, The University of Hong Kong, Hong Kong
[c] Department of Physics and Astronomy, University of Manitoba, Winnipeg, R3T 2N2, Canada
[d] Department of Physics and Materials Science, City University of Hong Kong, Hong Kong

ARTICLE INFO

Article history:
Received 30 May 2016
Received in revised form
7 August 2016
Accepted 17 August 2016
Available online xxx

Keywords:
Magnetic properties
SiTrO3 substrate
Thickness dependence

ABSTRACT

The exchange-coupled bilayers containing antiferromagnetic (AF) Cr_2O_3 have potential applications in novel spintronic devices with magneto-electric properties. The microstructures and magnetic properties of ion-beam sputtered NiFe/Cr_2O_3 bilayers are comparatively investigated at different Cr_2O_3 thicknesses on single-crystalline $SiTrO_3$ (STO) (001) and amorphous SiO_2 substrates. The formation of Cr_2O_3 is verified by X-ray photoelectron spectrometry. X-ray diffraction reveals a distinction in the preferred orientation of Cr_2O_3 deposited on different substrates. The variations in microstructure are responsible for the higher exchange bias, larger coercivity, and higher temperature stability of magnetization for samples grown on STO substrates. The coercivity and exchange bias at 10 K increases with Cr_2O_3 thickness. Higher Cr_2O_3 thickness also results in higher surface roughness, higher irreversibility temperature, and increased peak temperature of the out-of-phase AC susceptibility. This work has revealed the thickness dependence of the microstructure and magnetic properties of NiFe/Cr_2O_3 bilayers prepared on STO substrate. The outcome of this work may provide some insight for developing novel spintronic devices containing Cr_2O_3 and perovskite oxides.

1. Introduction

Exchange-coupled ferromagnetic/antiferromagnetic (FM/AF) bilayers are widely used in spin-valve based spintronic devices, such as hard disk reading heads, magnetoresistance sensors [1], magnetic random access memories (MRAM) [2], and spin-torque oscillators [3]. The coercivity (H_c) and exchange bias field (H_{ex}) can be tailored through modifying the exchange interaction in the FM/AF interfaces, enabling flexible control over the magnetic properties. The exchange coupling is influenced by a variety of factors such as temperature [4], layer thickness [5,6], interfacial qualities [7,8], and the domain structure [9] and composition of AF materials [10,11]. Cr_2O_3 is AF below 307 K [12–14] when Cr^{3+} spins are arranged antiparallel along the c axis [111] [15,16]. The AF order parameter of Cr_2O_3 can be switched by external electric field, enabling the magneto-electric (ME) switching of exchange coupling [12,15–17]. The application of Cr_2O_3 in exchange-biased multilayers will lead to novel spintronic devices with ME properties [18–20]. In these investigations, Cr_2O_3 epitaxially grown on single crystalline substrates is widely used for the high ME voltage coefficient. The ME properties can be induced in polycrystalline Cr_2O_3 through post-deposition field annealing [21–23]. This has enabled the fabrication of ME devices by a variety of methods on various substrates. Our previous research on NiFe/Cr-oxide bilayers deposited on SiO_2 and Al_2O_3 (0001) substrates has demonstrated modified magnetic properties by the substrate structure [24]. In-plane H_{ex} increases linearly with the thickness of Cr-oxide on the SiO_2 substrate, while the engagement of Al_2O_3 (0001) substrate has introduced out-of-plane exchange bias. $SiTrO_3$ (STO) is a high-k material that is widely used as a substrate in the preparation of perovskite oxides with various magnetic and electronic properties [25–27]. Asada et al. has shown that rhombohedral Cr_2O_3 can be

* Corresponding author.
** Corresponding author.
*** Corresponding author.
E-mail addresses: kwlin@dragon.nchu.edu.tw (K.-W. Lin), johan@physics.umanitoba.ca (J. van Lierop), ppong@eee.hku.hk (P.W.T. Pong).

http://dx.doi.org/10.1016/j.vacuum.2016.08.008
0042-207X/

formed on STO substrate with CeO_2 buffer layer [28]. However, the crystalline structures of Cr_2O_3 deposited directly on STO substrates are not yet reported. The thickness dependence of the microstructure and magnetic properties of FM/Cr_2O_3 bilayers grown on STO substrates remain unclear. The investigation on FM/Cr_2O_3 bilayers prepared on various substrates help to reveal the substrate effect of the properties of polycrystalline Cr_2O_3.

The dual ion beam deposition technique is a powerful sample fabrication method in which the chemical composition and surface quality of the layers can be manipulated through the bombardment of the End-Hall ion source [29–32]. This feature has offered great flexibility for the investigation of the exchange bias effect. In this work, dual ion beam sputtering is engaged to prepare NiFe/Cr_2O_3 bilayers on STO and SiO_2 substrates. The microstructures and magnetic properties are comparatively investigated to reveal the influence of STO substrate and AF-thickness on the bilayers' magnetism.

2. Materials and methods

NiFe/Cr_2O_3 bilayers were deposited on STO (001) substrates by dual ion-beam sputtering technique [33,34] at ambient temperature. The bottom Cr-oxide layer was prepared through in-situ oxidization during the deposition of Cr with an End-Hall ion source (V_{EH} = 70 V, 500 mA) with15% O_2/Ar ratio. The thickness of Cr-oxide layer was varied between 5.5 nm, 11 nm, 27.5 nm, and 55 nm. A 15-nm-thick NiFe layer was subsequently deposited using a Kaufman ion source (800 V, 7.5 mA) which was focused on a commercial $Ni_{80}Fe_{20}$ target. The base and working pressure were 3.9×10^{-7} and 6.5×10^{-4} mbar, respectively. A JEOL-2010 transmission electron microscope (TEM) operating at 200 kV was used to collect the planar and cross-sectional images. A ULVAC-PHI PHI 5000 Versa Probe X-ray photoelectron spectroscopy (XPS) was utilized to detect the depth profile of binding energy. A Brüker AXS D8 Advance grazing incidence (0.5°) X-ray diffraction (XRD) spectrometer was engaged in characterizing the crystalline structures. The topography and roughness were measured by a Bruker Dimension Icon atomic force microscope (AFM). Magnetic hysteresis loops were measured at 10 K by a superconducting quantum interference device (SQUID) magnetometer.

3. Results and discussion

The cross-sectional TEM images of NiFe/Cr_2O_3 (50 min)/STO are shown in Fig. 1(a). Sharp interfaces between Cr_2O_3 and STO are observed. A thin intermixing layer (~2 nm) is formed between NiFe and Cr_2O_3, as shown in the cross-sectional TEM and the depth profile of XPS in Fig. 1. (b). The XPS of Cr 2p and O 1s in the Cr-oxide layer (sputtering time = 3.65 min) are shown in Fig. 1 (c) and (d), respectively. The binding energy of 576.4 eV and 586 eV for Cr 2p [35] and ~530.2 eV for O 1s [36] indicates that Cr_2O_3 is formed during the bombardment.

The crystalline structures of bilayers deposited on STO and SiO_2 substrates were characterized by XRD as shown in Figs. 2 and 3, respectively. The major peak of NiFe (111) at $2\theta = 43.9°$ indicates that the lattice constant of the face-centered cubic (FCC) NiFe (3.55 Å) is not influenced by the thickness of Cr_2O_3 layer nor the different substrates. Rhombohedral Cr_2O_3 (110) peaks are observed at $2\theta = 36.2°$ in thick Cr_2O_3 layers grown on both substrates, and the lattice constants of hexagonal Cr_2O_3 are inferred to be 4.9 Å (a-axis) and 13.5 Å (c-axis). The poor (100) crystallinity in thin Cr_2O_3 layers is due to the amorphous nature of SiO_2 substrate or resulted from the large lattice mismatch (26%) between Cr_2O_3 (100) and STO (100) substrate. However, sharp Cr_2O_3 (211) peaks are observed at $2\theta = 57.6°$ in Fig. 2, which reveal a distinction in the preferred orientation in bilayers grown on single-crystalline STO substrates compared with those on the amorphous SiO_2 substrates. This is because the Cr_2O_3 (211) plane has smaller lattice mismatch with the STO (100) substrate. The substrate effect vanishes in the thickest Cr-oxide layer, since the ion-beam bombardment disorders the Cr_2O_3 (211) arrangement and establishes Cr_2O_3 (110) texture. From the XRD characterization, we can conclude that polycrystalline Cr_2O_3 can be formed on bare STO substrates. The crystalline phases are modified by the single-crystalline substrate.

The surface morphologies of NiFe/Cr_2O_3 5.5 nm/STO, NiFe/Cr_2O_3 27.5 nm/STO and NiFe/Cr_2O_3 55 nm/STO were characterized by AFM (Fig. 4). In each measurement, an area of 1 μm × 1 μm was scanned at the resolution of 256 × 256 pixels. The thin films grown on single-crystalline substrates are typically very smooth, due to the low roughness of the substrates (root mean square roughness (R_q) of 0.14 nm as reported in Ref. [37]). The ion bombardment during the Cr deposition also contributes to lower surface roughness [33]. With increasing Cr_2O_3 thickness, R_q gradually increases from 0.1 nm to 0.23 nm. This is likely due to the growth of Cr_2O_3 grains with increasing layer thickness.

The above results have shown that the STO substrates influence the bilayers by altering the preferred orientations of grains while the increasing Cr_2O_3 thickness modifies both crystalline structures and surface morphologies. SQUID measurements were subsequently conducted to investigate how the magnetic properties were modified by these structural changes. The hysteresis loops of bilayers grown on STO and SiO_2 substrates were measured at 10 K after field cooling (Fig. 5 (a) and (b), respectively). Square hysteresis loops are observed in all the samples, which is attributed to the enhanced ferromagnetism at cryogenic temperature. The curved edges and slightly reduced squareness (M_r/M_s decreasing from 0.99 to 0.95) in the hysteresis loops of NiFe/Cr_2O_3 55 nm/SiO_2 indicates enhanced exchange coupling in the bilayer. The establishment of exchange coupling is evidenced by the shifted hysteresis loop to the negative field. The observed exchange bias in polycrystalline-Cr_2O_3/NiFe [24,38,39] indicates that epitaxy of Cr_2O_3 is not necessary for introducing exchange interaction.

In order to gain insight on the thickness dependence of the magnetic properties, H_{ex} and H_c are plotted as a function of Cr_2O_3 thickness. The negative H_{ex} exhibits a trend to increase with Cr_2O_3 thickness (Fig. 6(a)). The enhanced exchange coupling when a thicker Cr_2O_3 layer is engaged is explained by the increased domain wall stability in Cr_2O_3 [40], the enhanced Cr_2O_3 (110) ordering, and the higher interfacial roughness [41] in the samples with thicker Cr_2O_3. The fluctuation in H_{ex}-thickness relation is attributed to the loop shift induced by the remnant field in the superconducting solenoid. The measured H_{ex} with SiO_2 substrates are smaller than that reported in Ref. [24] because thinner NiFe layers and annealed Cr-oxide layers are used in the previous investigation. The smaller FM thickness [42] and the annealing-induced AF ordering enhancement [24] contribute to higher H_{ex} in the previous paper. The intermixing in Cr_2O_3/NiFe interface also prevents the uncompensated spins from providing high unidirectional anisotropy to the FM layer. The H_{ex} of bilayers on SiO_2 substrates are smaller than those on STO substrates. As discussed in Figs. 2 and 3, the Cr_2O_3 exhibits (110) ordering on SiO_2 whereas it shows (211) ordering on STO. The atomic spins in Cr_2O_3(110) plane has larger magnetic form factor along the diagonal of the unit cell compared with the (211) plane [43]. This indicates that the Cr_2O_3 with (110) ordering has larger atomic magnetic moment [44] in each AF-aligned sub-lattice and thus stronger exchange interaction with the adjacent NiFe layer. H_c increases linearly with Cr_2O_3 thicknesses in the samples prepared on both substrates (Fig. 6(b)). The higher H_c in the samples with thicker Cr_2O_3 can be explained by the following two aspects. First, H_{ex} increases with Cr_2O_3 thickness, while higher H_{ex}

Please cite this article in press as: Y.-C. Chang, et al., Influence of Cr_2O_3 thickness on the magnetic properties of NiFe/Cr_2O_3 bilayers deposited on $SiTrO_3$ single-crystalline substrate, Vacuum (2016), http://dx.doi.org/10.1016/j.vacuum.2016.08.008

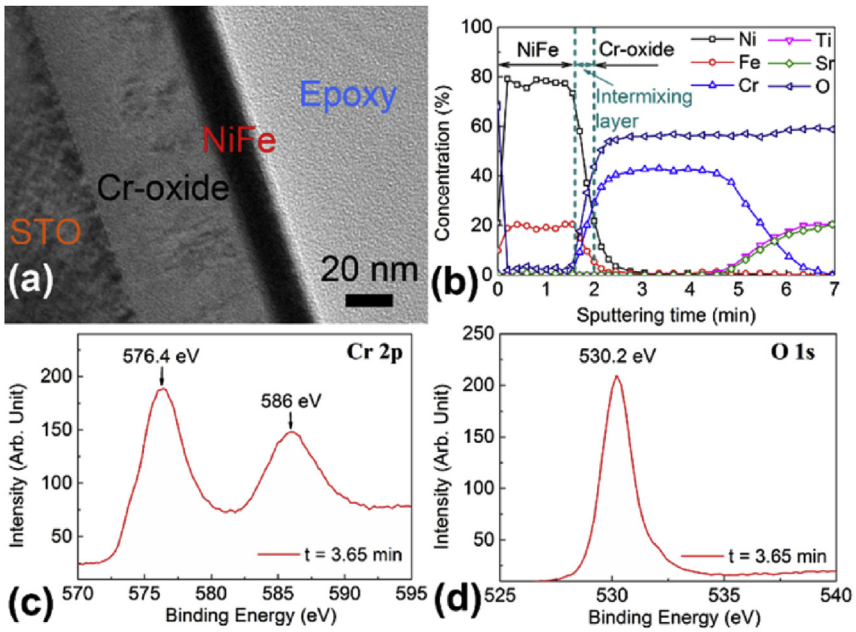

Fig. 1. (a) The cross-sectional TEM image, (b) the depth profile of elemental concentration, and the XPS of (c) Cr 2p and (d) O 1s in NiFe/Cr_2O_3 55 nm/STO.

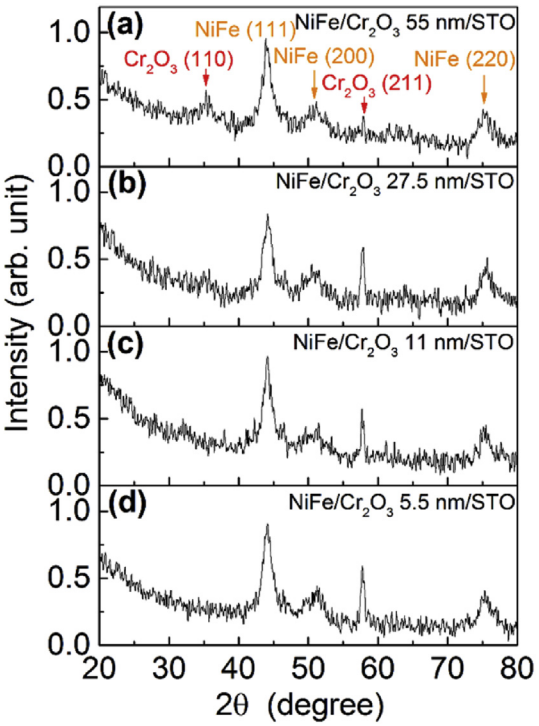

Fig. 2. The XRD patterns of bilayer deposited on STO (001) substrate with various Cr_2O_3 thicknesses (a) 55 nm (b) 27.5 nm (c) 11 nm, and (d) 5.5 nm.

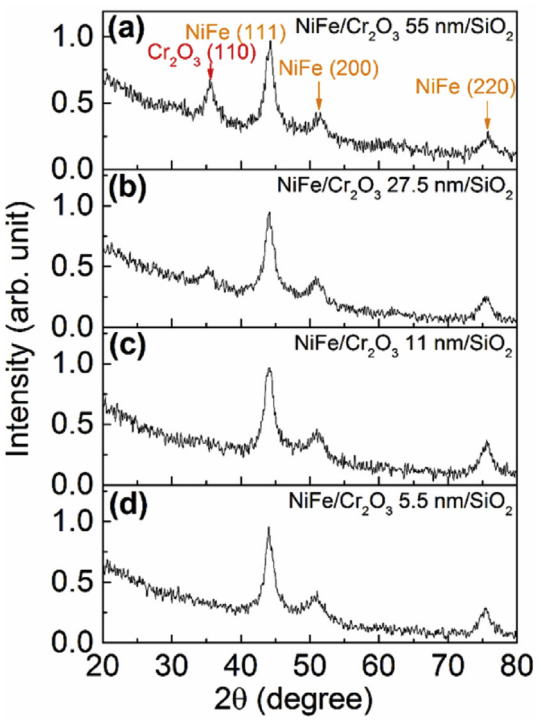

Fig. 3. The XRD patterns of bilayer deposited on SiO_2 substrate with various Cr_2O_3 thicknesses (a) 55 nm (b) 27.5 nm (c) 11 nm, and (d) 5.5 nm.

typically results in larger H_c [45]. Second, thicker Cr-oxides require ion bombardment of longer duration, which also induces more defects in the interfaces. These defects act as pinning sites in domain wall motion, which also contributes to the enhancing of H_c with increasing Cr-oxide thickness. The relatively larger H_c of the bilayers on SiO_2 substrates compared with STO substrates are consistent with the higher H_{ex} in these samples.

DC magnetometry measurements are conducted during the field cooling (FC) and zero-field cooling (ZFC) processes to reveal the temperature dependence of the bilayers' magnetism (Fig. 7). The bilayers deposited on both substrates show blocking temperature (T_b) of ~20–30 K, which is independent of Cr_2O_3 thickness. This indicates that exchange coupling is established when T < 20 K, which is also verified by the shift in the M-H loop at 10 K (Fig. 5). The measured T_b is far below the Neel temperature of Cr_2O_3 (307 K). The low T_b is possibly because of the finite thin film thickness and the disordered NiFe/Cr_2O_3 due to intermixing [46]. As a result, the thermal fluctuation should be reduced to a much smaller value to

Please cite this article in press as: Y.-C. Chang, et al., Influence of Cr_2O_3 thickness on the magnetic properties of NiFe/Cr_2O_3 bilayers deposited on $SiTrO_3$ single-crystalline substrate, Vacuum (2016), http://dx.doi.org/10.1016/j.vacuum.2016.08.008

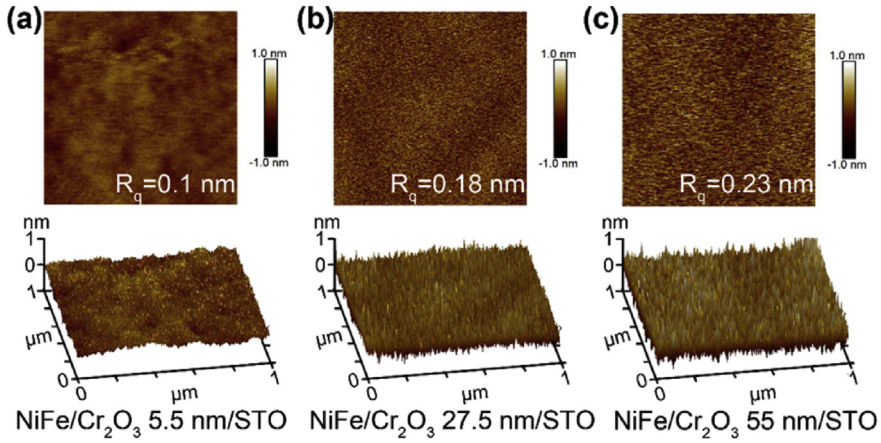

Fig. 4. The 2D and 3D morphologies and R_q of the bilayer with various Cr_2O_3 thicknesses deposited on STO (001) substrate (a) 5.5 nm (b) 27.5 nm (c) 55 nm.

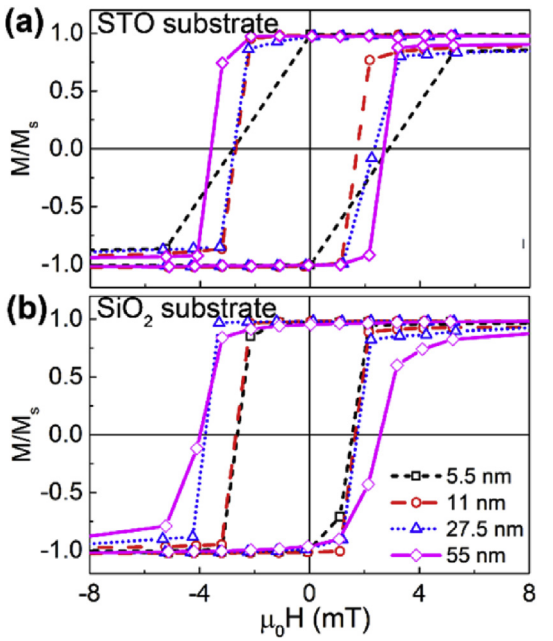

Fig. 5. The hysteresis loops of bilayer with various Cr_2O_3 thicknesses on (a) STO substrates and (b) SiO_2 substrates.

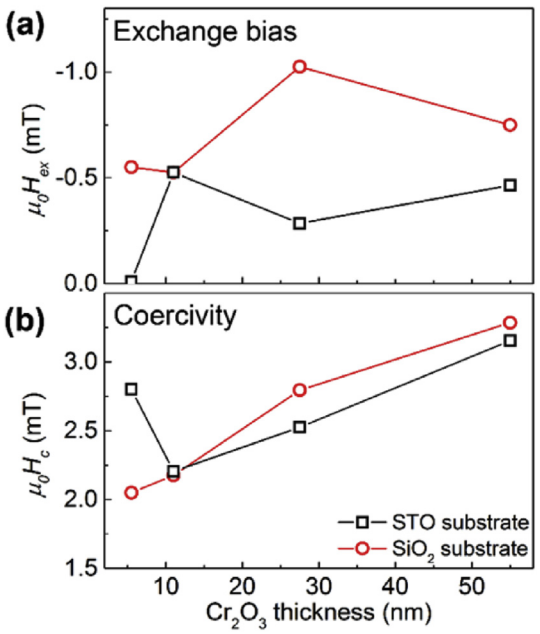

Fig. 6. (a) H_{ex} and (b) H_c as a function of Cr_2O_3 thickness in bilayers deposited on STO substrates and SiO_2 substrates.

maintain the AF ordering in Cr_2O_3 and to establish exchange coupling with NiFe. The irreversibility temperature (T_{irr}) represents the temperature where the frozen spin starts, and is calculated as the temperature where FC and ZFC curves diverge ($\Delta M = (M_{FC}-M_{ZFC})/M_{FC} > 1\%$ [47]). A gradual increase of the Cr_2O_3 thickness is observed in the samples deposited on both STO and SiO_2 substrates. This indicates that higher thermal energy is required to activate all the frozen spins of NiFe crystallite. The wider distribution of energy barrier with increasing Cr_2O_3 thickness shows that the magnetization of FM crystallites are also influenced by AF thickness. Highest T_{irr} of 250 K and 340 K are achieved in NiFe/Cr_2O_3 55 nm bilayers grown on STO and SiO_2 substrates, respectively. The strength of exchange coupling is quantitatively evaluated by the ΔM at 10 K [48]. As the thickness of Cr_2O_3 is increased from 5.5 nm to 55 nm, ΔM changes from 0.011 to 0.99 on STO substrates, and from 0.022 to 0.24 when SiO_2 substrates are used. This is consistent with the observation that H_{ex} increases with Cr_2O_3 thickness. It is noted that ΔM is smaller in NiFe/Cr_2O_3 55 nm/STO than in NiFe/Cr_2O_3 55 nm/SiO_2 above T_b. This indicates that the STO substrates alter and improve M(T) of the Cr_2O_3 layers by increasing its temperature stability.

The in-phase (χ'_{AC}) and out-of-phase (χ''_{AC}) AC susceptibility of NiFe/Cr_2O_3 5.5 nm/STO and NiFe/Cr_2O_3 11 nm/STO are plotted versus temperature in Fig. 8. The χ'_{AC} is a measure of the reversible magnetization process. At low temperatures (T < 20 K in NiFe/Cr_2O_3 5.5 nm/STO, and T < 70 K in NiFe/Cr_2O_3 11 nm/STO), the magnetic moments are locked into a static and ordered configuration [49], as evidenced by the low χ'_{AC}. As the temperature increases, the locked spins are activated by the thermal energy and start to fluctuate with the alternating magnetic field. The smaller χ'_{AC} in NiFe/Cr_2O_3 11 nm/STO results from the enhanced exchange coupling with the thicker AF layer, since χ'_{AC} is inversely proportional to the unidiactional anisotropy [50]. χ''_{AC} reflects the magnetic energy dissipation in the sample. The peak temperature of χ''_{AC} (240 K) in NiFe/Cr_2O_3 11 nm/STO is higher than that in NiFe/Cr_2O_3 5.5 nm/STO (40 K). The higher peak temperature and the higher onset

Please cite this article in press as: Y.-C. Chang, et al., Influence of Cr_2O_3 thickness on the magnetic properties of NiFe/Cr_2O_3 bilayers deposited on $SiTrO_3$ single-crystalline substrate, Vacuum (2016), http://dx.doi.org/10.1016/j.vacuum.2016.08.008

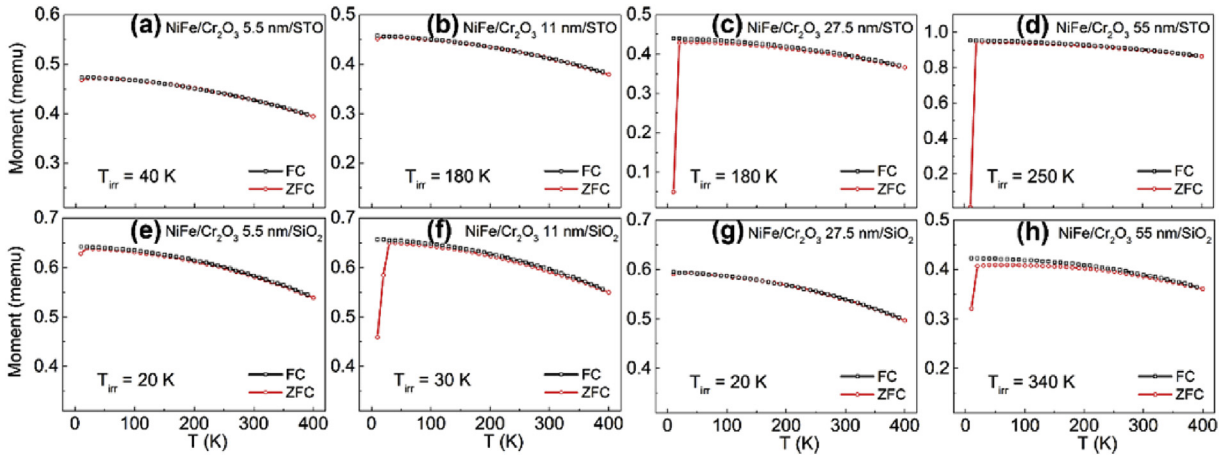

Fig. 7. The temperature dependent low-field magnetization of the bilayers under FC and ZFC with various Cr_2O_3 thickness on STO and SiO_2 substrates.

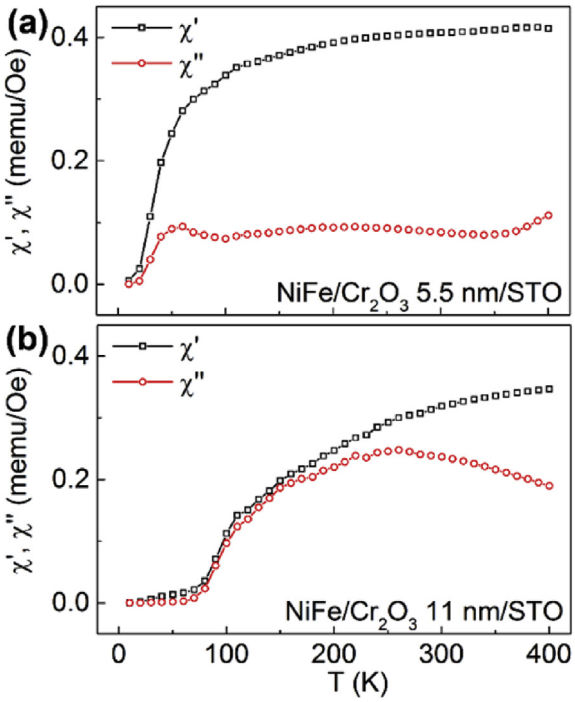

Fig. 8. The temperature dependence of the in-phase (χ'_{AC}) and out-of-phase (χ''_{AC}) AC susceptibility of bilayers with Cr_2O_3 thickness of (a) 5.5 nm and (b) 11 nm.

temperature for the locking of magnetic moments in NiFe/Cr_2O_3 11 nm/STO is consistent with the increased T_{irr} with Cr_2O_3 thickness observed in DC magnetometry (Fig. 7) [51].

4. Conclusions

The thickness dependence of the microstructures and magnetic properties of NiFe/Cr_2O_3 bilayers are investigated on single-crystalline STO substrates and are compared with that on SiO_2 substrates. Cr_2O_3 layers are formed by dual ion beam deposition, as characterized by XPS. The adoption of STO substrates changes the preferred orientation of Cr_2O_3 to (211), and this substrate effect diminishes with the increasing Cr-oxide thickness. The change in AF ordering is responsible for the smaller H_{ex} and H_c in hysteresis loops and higher temperature stability in M_{FC}/M_{ZFC} (T) of the bilayers prepared on STO substrates. While the Cr_2O_3 thickness is increased from 5.5 nm to 55 nm, enhanced Cr_2O_3 (110) ordering and increased surface roughness (from 0.1 nm to 0.23 nm) are observed. These structural changes result in enhanced $\mu_0 H_{ex}$ (from −0.1 mT to −0.5 mT) and increased $\mu_0 H_c$ (from ~2 mT to 3 mT) when STO substrates are used. Similar T_b of ~20 K is observed in all samples, which is attributed to the finite size effect and intermixing. T_{irr} increases with Cr_2O_3 thickness, which is also accompanied by the higher peak temperature in $\chi''_{AC}(T)$ curves. This work has shown that polycrystalline Cr_2O_3 can be directly grown on STO substrates. The revealed thickness dependence and substrate effect can be beneficial for evaluating the properties of multilayers containing Cr_2O_3. Further investigation is undergoing to explore the ME properties in field annealed polycrystalline-Cr_2O_3/FM bilayers prepared on different substrates.

Acknowledgments

This work was supported by the Ministry of Science and Technology (MOST) of Taiwan, the Natural Sciences and Engineering Research Council (NSERC) of Canada, the Seed Funding for Basic Research and Small Project Funding from the University of Hong Kong, the RGC-GRF grant (HKU 704911P), the ITF Tier 3 Fundings (ITS/104/13, ITS/214/14), and the University Grants Committee of Hong Kong (Contract No. AoE/P-04/08).

References

[1] C. Chappert, A. Fert, F.N. Van Dau, The emergence of spin electronics in data storage, Nat. Mater 6 (11) (2007) 813–823.
[2] E. Chen, D. Apalkov, Z. Diao, A. Driskill-Smith, D. Druist, D. Lottis, V. Nikitin, X. Tang, S. Watts, S. Wang, S.A. Wolf, A.W. Ghosh, J.W. Lu, S.J. Poon, M. Stan, W.H. Butler, S. Gupta, C.K.A. Mewes, T. Mewes, P.B. Visscher, Advances and future prospects of spin-transfer torque random access memory, IEEE Trans. Magn. 46 (6) (2010) 1873–1878.
[3] S.I. Kiselev, J.C. Sankey, I.N. Krivorotov, N.C. Emley, R.J. Schoelkopf, R.A. Buhrman, D.C. Ralph, Microwave oscillations of a nanomagnet driven by a spin-polarized current, Nature 425 (6956) (2003) 380–383.
[4] M.D. Stiles, R.D. McMichael, Temperature dependence of exchange bias in polycrystalline ferromagnet-antiferromagnet bilayers, Phys. Rev. B 60 (18) (1999) 12950.
[5] M. Ali, C.H. Marrows, M. Al-Jawad, B.J. Hickey, A. Misra, U. Nowak, K.D. Usadel, Antiferromagnetic layer thickness dependence of the IrMn/Co exchange-bias system, Phys. Rev. B 68 (21) (2003) 214420.
[6] K.-W. Lin, T.-C. Lan, C. Shueh, E. Skoropata, J. van Lierop, Modification of the ferromagnetic anisotropy and exchange bias field of NiFe/CoO/Co trilayers through the CoO spacer thicknesses, J. Appl. Phys. 115 (17) (2014) 17D717.
[7] J. Kanak, T. Stobiecki, S. van Dijken, Influence of interface roughness, film texture, and magnetic anisotropy on exchange bias in $[Pt/Co]_3$/IrMn and IrMn $[Co/Pt]_3$/Multilayers, IEEE Trans. Magn. 44 (2) (2008) 238–245.

Please cite this article in press as: Y.-C. Chang, et al., Influence of Cr_2O_3 thickness on the magnetic properties of NiFe/Cr_2O_3 bilayers deposited on $SiTrO_3$ single-crystalline substrate, Vacuum (2016), http://dx.doi.org/10.1016/j.vacuum.2016.08.008

[8] K.D. Usadel, R.L. Stamps, Exchange bias: dependence on the properties of the ferromagnetic interface layer, Phys. Rev. B 82 (9) (2010) 094432.
[9] A. Fraile Rodríguez, A.C. Basaran, R. Morales, M. Kovylina, J. Llobet, X. Borrisé, M.A. Marcus, A. Scholl, I.K. Schuller, X. Batlle, A. Labarta, Manipulation of competing ferromagnetic and antiferromagnetic domains in exchange-biased nanostructures, Phys. Rev. B 92 (17) (2015) 174417.
[10] K.W. Lin, R.J. Gambino, L.H. Lewis, Structural and magnetic characterization of ion-beam deposited NiFe/NixFe1-xO composite films, J. Appl. Phys. 93 (10) (2003) 6590–6592.
[11] X. Li, K.W. Lin, H.Y. Liu, D.H. Wei, G.J. Li, P.W.T. Pong, Effect of field cooling process and ion-beam bombardment on the exchange bias of NiCo/(Ni, Co)O bilayers, Thin Solid Films 570 (2014) 383–389.
[12] X. Chen, A. Hochstrat, P. Borisov, W. Kleemann, Magnetoelectric exchange bias systems in spintronics, Appl. Phys. Lett. 89 (20) (2006) 202508.
[13] M. Bibes, A. Barthelemy, Multiferroics: towards a magnetoelectric memory, Nat. Mater 7 (6) (2008) 425–426.
[14] W. Kleemann, Magnetoelectric spintronics, J. Appl. Phys. 114 (2) (2013) 027013.
[15] D. Astrov, The magnetoelectric effect in antiferromagnetics, Sov. Phys. JETP 11 (3) (1960) 708–709.
[16] D. Astrov, Magnetoelectric effect in chromium oxide, Sov. Phys. JETP 13 (4) (1961) 729–733.
[17] P. Borisov, A. Hochstrat, X. Chen, W. Kleemann, C. Binek, Magnetoelectric switching of exchange bias, Phys. Rev. Lett. 94 (11) (2005) 117203.
[18] P. Borisov, A. Hochstrat, V. Shvartsman, W. Kleemann, T. Eimüller, A.F. Rodríguez, Thin Cr2O3 films for magnetoelectric data storage deposited by reactive e-beam evaporation, Ferroelectrics 370 (1) (2008) 147–152.
[19] S. Fusil, V. Garcia, A. Barthélémy, M. Bibes, Magnetoelectric devices for spintronics, Annu. Rev. Mater. Res. 44 (1) (2014) 91–116.
[20] W. Echtenkamp, C. Binek, Electric control of exchange bias training, Phys. Rev. Lett. 111 (18) (2013) 187204.
[21] Y.Y. Liu, S.H. Xie, J.Y. Li, The effective medium approximation for annealed magnetoelectric polycrystals, J. Appl. Phys. 103 (2) (2008) 023919.
[22] Y.Y. Liu, S.H. Xie, G. Jin, J.Y. Li, The effective magnetoelectric coefficients of polycrystalline Cr2O3 annealed in perpendicular electric and magnetic fields, J. Appl. Phys. 105 (7) (2009) 073917.
[23] J. Ryu, S. Priya, K. Uchino, H.-E. Kim, Magnetoelectric effect in composites of magnetostrictive and piezoelectric materials, J. Electroceram 8 (2) (2002) 107–119.
[24] K.-W. Lin, J.-Y. Guo, Tuning in-plane and out-of-plane exchange biases in Ni80Fe20/Cr-oxide bilayers, J. Appl. Phys. 104 (12) (2008) 123913.
[25] B.K. Choudhury, K.V. Rao, R.N.P. Choudhury, Dielectric properties of SrTiO3 single crystals subjected to high electric fields and later irradiated with X-rays orγ-rays, J. Mater. Sci. 24 (10) (1989) 3469–3474.
[26] H. Chen, A.M. Kolpak, S. Ismail-Beigi, Electronic and magnetic properties of SrTiO3/LaAlO3 interfaces from first principles, Adv. Mater 22 (26–27) (2010) 2881–2899.
[27] H. Lu, T.A. George, Y. Wang, I. Ketsman, J.D. Burton, C.-W. Bark, S. Ryu, D.J. Kim, J. Wang, C. Binek, P.A. Dowben, A. Sokolov, C.-B. Eom, E.Y. Tsymbal, A. Gruverman, Electric modulation of magnetization at the BaTiO3/La0.67Sr0.33MnO3 interfaces, Appl. Phys. Lett. 100 (23) (2012) 232904.
[28] A. Takeshi, N. Kenjirou, I. Nobuyuki, Y. Hiroshi, Crystal growth of magnetoelectric Cr2O3 thin film on sapphire and SrTiO3, Jpn. J. Appl. Phys. 47 (1S) (2008) 546.
[29] X. Li, K.W. Lin, H.T. Liang, H.F. Hsu, N.G. Galkin, Y. Wroczynskyj, J. van Lierop, P.W.T. Pong, The effects of interfacial interactions between Fe–O and Fe–Si induced by ion-beam bombardment on the magnetic properties of Si-oxide/Fe bilayers, Nucl. Instrum. Methods. Phys. Res. B 365 (2015) 196–201.
[30] X. Li, K.W. Lin, H.T. Liang, P.L. Liu, W.C. Lo, D.L. Cortie, F. Klose, J. van Lierop, L. Li, P.W.T. Pong, The effects of post-deposition ion-beam bombardment with oxygen on the Co surface in modifying the magnetic properties of Co thin films, Microelectron. Eng. 152 (2016) 41–47.
[31] C. Zheng, T.-C. Lan, C. Shueh, R.D. Desautels, J.v. Lierop, K.-W. Lin, P.W.T. Pong, Effect of ion-beam bombardment on microstructural and magnetic properties of Ni 80 Fe 20/α-Fe 2 O 3 thin films, Jpn. J. Appl. Phys. 53 (6S) (2014), 06JB03.
[32] C. Zheng, K.-W. Lin, C.-H. Liu, H.-F. Hsu, C.-W. Leung, W.-H. Chen, T.-H. Wu, R.D. Desautels, J. van Lierop, P.W.T. Pong, Microstructural and magnetic characterization of ion-beam bombarded [Ni80Fe20-Cr]50 thin films, Vacuum 118 (2015) 85–89.
[33] K.W. Lin, M. Mirza, C. Shueh, H.R. Huang, H.F. Hsu, J. van Lierop, Tailoring interfacial exchange coupling with low-energy ion beam bombardment: tuning the interface roughness, Appl. Phys. Lett. 100 (12) (2012) 122409.
[34] H.R. Kaufman, R.S. Robinson, R.I. Seddon, End-Hall ion source, J. Vac. Sci. Technol. A 5 (4) (1987) 2081–2084.
[35] G.C. Allen, S.J. Harris, J.A. Jutson, J.M. Dyke, A study of a number of mixed transition metal oxide spinels using X-ray photoelectron spectroscopy, Appl. Surf. Sci. 37 (1) (1989) 111–134.
[36] E. Paparazzo, XPS analysis of oxides, Surf. Interface Anal. 12 (2) (1988) 115–118.
[37] D. Dale, A. Fleet, Y. Suzuki, J.D. Brock, X-ray scattering from real surfaces: discrete and continuous components of roughness, Phys. Rev. B 74 (8) (2006) 085419.
[38] X.H. Liu, W. Liu, S. Guo, F. Yang, X.K. Lv, W.J. Gong, Z.D. Zhang, Effects of anisotropy and spin-asymmetry of ferromagnetic materials in ferromagnetic/Cr2O3/ferromagnetic trilayers, Appl. Phys. Lett. 96 (8) (2010) 082501.
[39] X.H. Liu, W. Liu, S. Guo, X.K. Lv, W.J. Gong, Z.D. Zhang, Competition between interfacial and interlayer exchange couplings in Co/Cr2O3/Fe trilayers, J. Alloy. Compd. 509 (5) (2011) 1448–1451.
[40] K.W. Lin, J.Y. Guo, H.Y. Liu, H. Ouyang, Y.L. Chan, D.H. Wei, J. van Lierop, Anomalous exchange bias behavior in ion-beam bombarded NiCo/(Ni,Co)O bilayers, J. Appl. Phys. 103 (7) (2008) 07C105.
[41] D.C. Parks, P.J. Chen, W.F. Egelhoff, R.D. Gomez, Interfacial roughness effects on interlayer coupling in spin valves grown on different seed layers, J. Appl. Phys. 87 (6) (2000) 3023–3026.
[42] T. Lin, T. Ching, R.E. Fontana, J.K. Howard, Exchange-coupled Ni-Fe/Fe-Mn, Ni-Fe/Ni-Mn and NiO/Ni-Fe films for stabilization of magnetoresistive sensors, IEEE Trans. Magn. 31 (6) (1995) 2585–2590.
[43] B.N. Brockhouse, Antiferromagnetic structure in Cr2O3, J. Chem. Phys. 21 (5) (1953) 961–962.
[44] C.G. Shull, W.A. Strauser, E.O. Wollan, Neutron diffraction by paramagnetic and antiferromagnetic substances, Phys. Rev. 83 (2) (1951) 333–345.
[45] J. Nogués, I.K. Schuller, Exchange bias, J. Magn. Magn. Mater 192 (2) (1999) 203.
[46] I.O. Dzhun, S.A. Dushenko, N.G. Chechenin, E.A. Konstantinova, Temperature dependence of exchange bias in Co/FeMn-structure induced by heating and cooling in magnetic field, J. Phys. Conf. Ser. 303 (1) (2011) 012103.
[47] P. Zhang, F. Zuo, F.K. Urban Iii, A. Khabari, P. Griffiths, A. Hosseini-Tehrani, Irreversible magnetization in nickel nanoparticles, J. Magn. Magn. Mater 225 (3) (2001) 337–345.
[48] K.-W. Lin, C. Shueh, C.-H. Liu, E. Skoropata, T.-H. Wu, J. van Lierop, Using different Mn-oxides to influence the magnetic anisotropy of FePt in bilayers with little change of the exchange bias field, J. Appl. Phys. 113 (17) (2013), 17C104.
[49] J. van Lierop, K.W. Lin, J.Y. Guo, H. Ouyang, B.W. Southern, Proximity effects in an exchange-biased Ni80Fe20/Co3O4 thin film, Phys. Rev. B 75 (13) (2007) 134409.
[50] J. Åkerman, V. Ström, K.V. Rao, E.D. Dahlberg, Separation of exchange anisotropy and magnetocrystalline anisotropy in CoO bilayers by means of ac susceptibility measurements, Phys. Rev. B 76 (14) (2007) 144416.
[51] D.N.H. Nam, K. Jonason, P. Nordblad, N.V. Khiem, N.X. Phuc, Coexistence of ferromagnetic and glassy behavior in the La0.5Sr0.5CoO3 perovskite compound, Phys. Rev. B 59 (6) (1999) 4189–4194.

Please cite this article in press as: Y.-C. Chang, et al., Influence of Cr_2O_3 thickness on the magnetic properties of NiFe/Cr_2O_3 bilayers deposited on $SiTrO_3$ single-crystalline substrate, Vacuum (2016), http://dx.doi.org/10.1016/j.vacuum.2016.08.008